# Half-metallicity and magnetism of GeTe doped with transition metals V, Cr and Mn: a theoretical study from the viewpoint of application in spintronics

Y. Liu

*College of Science, Yanshan University, Qinhuangdao, Hebei 066004,*
*China; Physics Department, Brock University, St. Catharines, Ontario L2S 3A1, CANADA*

S.K. Bose*

*Physics Department, Brock University, St. Catharines, Ontario L2S 3A1, CANADA*

J. Kudrnovský

*Institute of Physics, Academy of the Sciences of the Czech Republic,*
*Na Slovance 2, 182 21 Prague 8, Czech Republic*

This work presents results for the magnetic properties of the compound GeTe doped with $3d$ transition metals V, Cr and Mn from the viewpoint of potential application in spintronics. We report a systematic density-functional study of the electronic structure, magnetic and cohesive properties of these ternary compounds in both rock salt and zinc blende structures. In both cases, it is the Ge sublattice that is doped with the three transition metals. Some of these compounds are found to be half-metallic at their optimized cell volumes. For these particular cases, we calculate both exchange interactions and the Curie temperatures in order to provide some theoretical guidance to experimentalists trying to fabricate materials suitable for spintronic devices. Discussions relating our results to the existing experimental studies are provided whenever applicable and appropriate. Apparent discrepancy between experimental observations and our theoretical result for the case of Mn-doping is discussed in detail, pointing out various physical reasons and possible resolutions of the apparent discrepancy.

arXiv:1209.1063v1 [cond-mat.mtrl-sci] 5 Sep 2012

## I. INTRODUCTION

In recent years GeTe thin films doped with $3d$ transition metals have received considerable attention from experimentalists interested in the field of magnetic semiconductors.[1–8] Ferromagnetic order was observed for the Cr, Mn, and Fe doped films, whereas Ti, V, Co and Ni doped films were found to be paramagnetic.[2] The Curie temperatures $T_c$ of these thin films have been found to depend on the type and concentration of the dopants, with a high value of 140 K, reported for $Ge_{1-x}Mn_xTe$ for $x=0.51$.[1] Later on this group of researchers reported even higher value of $T_c \sim 190$ K in dilute magnetic semiconductor (DMS) $Ge_{0.92}Mn_{0.08}Te$.[7] $T_c$s around 200-250 K have been reported by Fukuma *et al.*[5] for $Ge_{1-x}Cr_xTe$ thin films for low values of $x$ ($\leq 0.1$). The thin films in all these studies were of predominantly rock salt structure. For spintronic applications, the desired properties of such ferromagnets are half-metallicity and relatively high Curie temperatures. Possibility of half-metallicity in Cr- and V-substituted GeTe bulk compounds has been reported by Zhao *et al.*,[9] based on theoretical calculations using linear augmented plane waves (LAPW) WIEN2k code for some ordered Ge-V-Te and Ge-Cr-Te compounds. These authors left the issue of the Curie temperature unattended, as only the electronic band structure, density of states and charge density were studied, and not the exchange interaction in these compounds. A theoretical study of the electronic structure of $Ge_{1-x}Mn_xTe$, based on the generalized gradient approximation plus Hubbard U (GGA+U), has been presented by Ciucivara *et al.*[10] Among the magnetic properties only the magnetic moment was considered, the issue of the exchange interaction and $T_c$ was not addressed. Recently a large number of experimental studies related to magnetism and magnetic transitions in several Ge-Te based alloys, such as Ge-Cr-Te, Ge-Mn-Te and Ge-Fe-Te) have been reported.[11–21] In addition, there is substantial amount work on DMSs in general (for a review see [22]), where the magnetic properties arise via percolation effects among a very small concentration of the magnetic atoms. For a discussion on magnetic percolation in DMSs readers may consult the work by Bergqvist *et al.*[23]

In view of the large body of existing experimental work as mentioned above, we have embarked on a systematic theoretical study of the GeTe system doped with $3d$ transition metal atoms. The most commonly occurring structure for both bulk and thin films of these compounds is the NaCl or the rock-salt (RS) structure. However, from the theoretical viewpoint an equally interesting structure to study is the zinc blende (ZB) structure. Both RS and ZB are fcc-based, but differ in terms of the distance between the Ge and Te atoms. Thus irrespective of whether one dopes the Te- or the Ge-sublattice with a magnetic ($3d$) atom, the magnetic effects are expected to differ because of different levels of hybridization between the $3d$ orbitals and the $s$ and $p$ orbitals of the Ge or Te atoms. Experimentally it may be possible to grow both RS and ZB structures, even though the ground state structure appears to be RS. Thus we have studied the electronic

and magnetic properties of both these structures for different concentrations of the magnetic V, Cr, and Mn atoms. We have employed supercell method as well as the coherent potential approximation (CPA) to study the effect of doping at various concentrations. The supercell calculations are carried out using the full potential linear augmented plane wave (FP-LAPW) method using the WIEN2k code.[24] The CPA calculations are carried out within the frame-work of the linear muffin-tin orbital (LMTO) method using the atomic sphere approximation (ASA).[25,26] In a limited number of cases, when the half-metallicity is predicted on the basis of both supercell and CPA calculations, we have provided results for exchange interactions and Curie temperatures for these alloys.

## II. COMPUTATIONAL DETAILS

The crystal structures of the ternary GeTe based compounds $Ge_{1-x}TM_xTe$ (TM stands for transition metal atoms V, Cr and Mn) were constructed from the unit cell of RS and ZB structures as follows. The doping levels of x=0.25 or 0.75 were achieved by replacing the Ge atoms at the vertex site or face-center sites, respectively, of the RS/ZB unit cell , with the TM atoms. Both cases (x=0.25 or 0.75) have the same space group ($Pm\bar{3}m$, or 221) for the RS structure, and ($P\bar{4}3m$, or 215) for ZB. The x=0.5 doping is obtained by replacing the Ge atoms at the four compatible face-center sites. In this way we generate tetragonal structure ($P\bar{4}m2$, 115) for the ZB case and ($P4/mmm$, 123) for RS. This procedure of realizing the doping levels results in minimal primitive cells, with the highest possible symmetry. Numerous semiconductors are known to crystallize in the ZB or RS structures. As such these ternary compounds should be compatible with a large number of semiconductors.

Calculations were carried out within the framework of the density-functional theory (DFT),[27] using the WIEN2k[24] code based on the full-potential linear augmented plane wave plus local orbitals method. The generalized gradient approximation (GGA) proposed by Perdew *et al.* was used for exchange and correlation potentials.[28,29] We consider full relativistic effects for the core states and use the scalar-relativistic approximation for the valence states, neglecting the spin-orbit coupling. The latter is known to produce only a small effect on the results that are of interest in this work, e.g., density of states and the energy gaps.

As a note to practitioners of this code, we used 3000 K points (Monkhorst-Park grid)[30] for the Brillouin-zone integration, set $Rmt * Kmax = 8.0$ and carried out the angular momentum expansion up to $l_{max} = 10$ in the muffin tins, and used $G_{max} = 14$ for the charge density. All core and valence states are treated self-consistently. Convergence with respect to basis set and k-point sampling was carefully verified. The self-consistent calculation is allowed to stop only when the integrated charge difference per formula unit, $\int |\rho_n - \rho_{n-1}| dr$, for the input and output charge densities $\rho_{n-1}$ and $\rho_n$ is less than $10^{-4}$. In the calculation of Ge-X-Te in different structures, the muffin-tin (MT) radii are chosen to be 2.3, 2.2 and 2.5 a.u. for Ge, X (X=V, Cr, Mn) and Te atoms, respectively.

## III. ELECTRONIC STRUCTURE

### A. Results of supercell calculations using the FP-LAPW method

For each case equilibrium lattice parameter was obtained by minimizing the total energy with respect to the cell volume. All electronic properties such as the density of states (DOS), energy bands and magnetic moments were then calculated for the equilibrium lattice parameters. Among all the ternary TM compounds with the doping levels considered, we find 9 half-metallic (HM) cases: one Mn-doped, three Cr-doped, and three V-doped cases for the RS structure; and one Cr-doped and one V-doped cases for the ZB structure (see Tables I-IV). There is a small drop in the value of the equilibrium lattice parameter with increasing dopant concentration in all cases. This is supported by the measurements of lattice parameters for the thin films of $Ge_{1-x}Mn_xTe$ and $Ge_{1-x}Cr_xTe$ grown in RS structure.[1,5] Bulk moduli, calculated by using Birch-Murnaghan equation of state,[31] are found to increase with the doping level for V- and Cr-doping. For Mn-doping this change is non-monotonic. The equilibrium lattice constants, X-Te bond lengths, and bulk moduli, magnetic moments, minority-spin gaps, and half-metallic gaps for the ternary compounds in RS structure are summarized in Tables I and II. The same quantities for the ternary compounds in ZB structure are summarized in Tables III and IV. In general, the band gap tends to increase with decreasing lattice parameter. This is understandable as the increased hybridization due to decreasing inter-atomic distances leads to increased separation between the energies of the bonding and anti-bonding states.

Tables II and IV show that most of the moments are associated with the muffin-tins around the TM atoms and the interstitial space. The orbitals associated with Ge and Te atoms have little spin polarization. While the values of the TM and interstitial moments are dependent on the muffin-tin radii, the integer values of the total moments shown in the last column clearly identify the half-metallic cases.

Note that in all cases studied and reported in Tables I-IV, the RS structure has lower energy than the ZB, indicating the equilibrium bulk phase to be RS at low temperatures. However, it might be possible to grow thin films of these compounds in ZB structure under suitable conditions. Therefore, there is some merit in comparing the magnetic properties of these two fcc-based phases. So far all thin films of these compounds seem to have been grown in RS structure or with small rhombohedral

TABLE I: Results obtained via the WIEN2k code for the RS compounds $Ge_{4-n}X_nTe_4$ (X=V,Cr,Mn) : the equilibrium lattice constants $a$, the X-Te bond length $L_{XTe}$, bulk modulus $B$, minority-spin gaps $G_{MIS}$ (eV), and half-metallic gaps $G_{HM}$ (eV). All results shown are obtained using GGA (see text).

| compounds | $a$(Å) | $L$(Å) | $B$(GPa) | $G_{MIS}$(eV) | $G_{HM}$(eV) |
|---|---|---|---|---|---|
| $Ge_3V_1Te_4$ | 5.9283 | 2.9642 | 51.3 | 0.599 | 0.097 |
| $Ge_2V_2Te_4$ | 5.8497 | 2.9249 | 55.8 | 0.816 | 0.170 |
| $Ge_1V_3Te_4$ | 5.7865 | 2.8933 | 59.7 | 1.007 | 0.213 |
| $Ge_3Cr_1Te_4$ | 5.9325 | 2.9662 | 51.4 | 0.571 | 0.220 |
| $Ge_2Cr_2Te_4$ | 5.8579 | 2.9290 | 54.9 | 0.789 | 0.382 |
| $Ge_1Cr_3Te_4$ | 5.7860 | 2.8930 | 58.2 | 0.980 | 0.371 |
| $Ge_3Mn_1Te_4$ | 5.9638 | 2.9819 | 49.7 | 0.710 | 0.200 |
| $Ge_2Mn_2Te_4$ | 5.9139 | 2.9568 | 46.1 | - | - |
| $Ge_1Mn_3Te_4$ | 5.8413 | 2.9206 | 43.1 | - | - |

TABLE III: Results obtained via the WIEN2k code for the ZB compounds $Ge_{4-n}X_nTe_4$ (X=V,Cr,Mn) : the equilibrium lattice constants $a$, the X-Te bond length $L_{XTe}$, bulk modulus $B$, minority-spin gaps $G_{MIS}$ (eV), and half-metallic gaps $G_{HM}$ (eV). All results shown are obtained using GGA (see text).

| compounds | a(Å) | L(Å) | B(GPa) | $G_{MIS}$(eV) | $G_{HM}$(eV) |
|---|---|---|---|---|---|
| $Ge_3V_1Te_4$ | 6.5842 | 2.8510 | 27.7 | - | - |
| $Ge_2V_2Te_4$ | 6.4316 | 2.7953 | 33.8 | - | - |
| $Ge_1V_3Te_4$ | 6.3109 | 2.7327 | 42.2 | 1.061 | 0.482 |
| $Ge_3Cr_1Te_4$ | 6.5950 | 2.8556 | 30.4 | - | - |
| $Ge_2Cr_2Te_4$ | 6.4347 | 2.7866 | 34.0 | - | - |
| $Ge_1Cr_3Te_4$ | 6.3280 | 2.7401 | 38.8 | 1.144 | 0.253 |
| $Ge_3Mn_1Te_4$ | 6.6405 | 2.8754 | 29.1 | - | - |
| $Ge_2Mn_2Te_4$ | 6.5305 | 2.8281 | 30.1 | - | - |
| $Ge_1Mn_3Te_4$ | 6.4222 | 2.7809 | 26.5 | - | - |

TABLE II: Magnetic moment per magnetic atom (f.u.) in units of bohr magneton $\mu_B$, for the RS compounds $Ge_{4-n}X_nTe_4$ (X=V, Cr, Mn), at their respective equilibrium volumes, obtained by using the FP-LAPW method (WIEN2k). Moments associated with X, Te, Ge muffin-tin spheres and the interstitial region (Int) are shown separately.

| compounds | $X(\mu_B)$ | $Te(\mu_B)$ | $Ge(\mu_B)$ | $Int(\mu_B)$ | Tot $(\mu_B)$ |
|---|---|---|---|---|---|
| $Ge_3V_1Te_4$ | 2.463 | -0.050 | 0.026 | 0.624 | 3.000 |
| $Ge_2V_2Te_4$ | 2.482 | -0.053 | 0.043 | 0.606 | 3.000 |
| $Ge_1V_3Te_4$ | 2.497 | -0.076 | 0.048 | 0.589 | 3.000 |
| $Ge_3Cr_1Te_4$ | 3.580 | -0.065 | 0.017 | 0.576 | 4.000 |
| $Ge_2Cr_2Te_4$ | 3.575 | -0.065 | 0.031 | 0.565 | 4.000 |
| $Ge_1Cr_3Te_4$ | 3.567 | -0.120 | 0.047 | 0.558 | 4.000 |
| $Ge_3Mn_1Te_4$ | 4.243 | 0.035 | 0.024 | 0.583 | 5.000 |
| $Ge_2Mn_2Te_4$ | 4.226 | 0.032 | 0.053 | 0.561 | 4.947 |
| $Ge_1Mn_3Te_4$ | 4.140 | 0.050 | 0.083 | 0.494 | 4.167 |

TABLE IV: Magnetic moment per magnetic atom (f.u.) in units of bohr magneton $\mu_B$, for the ZB compounds $Ge_{4-n}X_nTe_4$ (X=V, Cr, Mn), at their respective equilibrium volumes, obtained by using the FP-LAPW method (WIEN2k). Moments associated with X, Te, Ge muffin-tin spheres and the interstitial region (Int) are shown separately.

| compounds | $X (\mu_B)$ | $Te(\mu_B)$ | $Ge(\mu_B)$ | $Int(\mu_B)$ | $Tot(\mu_B)$ |
|---|---|---|---|---|---|
| $Ge_3V_1Te_4$ | 2.535 | -0.079 | 0.022 | 0.719 | 3.007 |
| $Ge_2V_2Te_4$ | 2.510 | -0.109 | 0.027 | 0.690 | 3.009 |
| $Ge_1V_3Te_4$ | 2.463 | -0.113 | 0.040 | 0.674 | 3.000 |
| $Ge_3Cr_1Te_4$ | 3.706 | -0.079 | 0.013 | 0.675 | 4.103 |
| $Ge_2Cr_2Te_4$ | 3.625 | -0.126 | 0.014 | 0.658 | 4.045 |
| $Ge_1Cr_3Te_4$ | 3.560 | -0.145 | 0.021 | 0.627 | 4.000 |
| $Ge_3Mn_1Te_4$ | 4.171 | 0.024 | 0.033 | 0.634 | 5.003 |
| $Ge_2Mn_2Te_4$ | 4.190 | 0.054 | 0.068 | 0.635 | 5.002 |
| $Ge_1Mn_3Te_4$ | 4.191 | 0.056 | 0.078 | 0.597 | 4.889 |

distortions from this structure.[1,2,7,15]

The densities of states for some these ordered compounds at their equilibrium lattice parameters are shown in Figs.(1-2). These results clearly show in which cases half-metallicity is most robust, i.e. the Fermi level is most widely separated from the band edges. The partial atom-projected densities of states shown for $Ge_2V_2Te_4$, shows that the states at the Fermi level have a high TM character. The situation should be similar for TM=Cr, Mn as well, with the amount of the TM character changing with TM concentration. The 25% Mn-doping case needs special attention, since the metallic character is either marginal (ZB structure) or absent (RS structure). For Ge-Te in the ZB structure, 25% Mn-doping of the Ge-sublattice produces a borderline, i.e., zero gap, semiconductor or semimetal. For the RS-structure, the same Mn-doping level of the Ge-sublattice produces a narrow gap semiconductor. As we will see in the next section, the nature of magnetism in these compounds is dictated by the availability of free carriers or holes. Thus the Mn-doping case will be considered in some additional detail.

The results presented in Tables I-IV and Figs. 1-2 are for ordered alloys, while the TM-doped thin films of GeTe are partially random, in the sense that the Ge-sublattice sites are occupied randomly by Ge and TM atoms. We have studied the electronic structure of these partially random alloys using the tight-binding linear muffin-tin orbital(TB-LMTO) method in conjunction with the CPA.[25,26] These calculations employed exchange-correlation potential of Vosko, Wilk and Nusair,[32] an $s, p, d, f$ basis set, relativistic treatment of
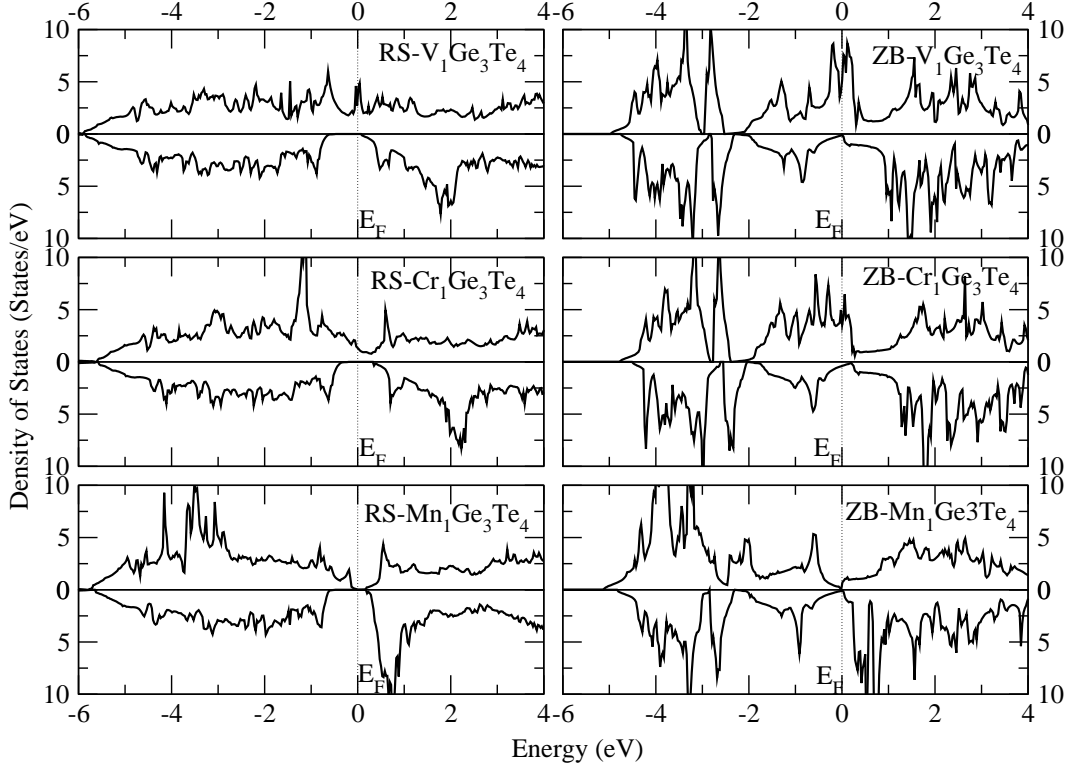
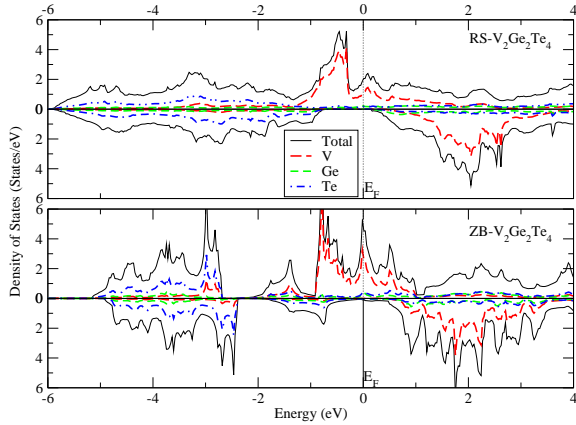FIG. 1: Densities of states in $Ge_3TM_1Te_4$ (TM=V,Cr,Mn) alloys in RS and ZB structures.



FIG. 2: (Color online) Total and component-resolved densities of states in $V_2Ge_2Te_4$ alloys in RS and ZB structures.

core electrons and scalar-relativistic treatment of valence electrons. The results, particularly with respect to half-metallicity, were similar to those of the ordered alloys, apart from expected smoothing of some peaks in the DOS. The gaps values were marginally lower and can be

ascribed to the differences between local density approximation (LDA) in TB-LMTO and GGA in FP-LAPW. The equilibrium lattice parameters were 2-4% higher in TB-LMTO LDA calculations.

## IV. EXCHANGE INTERACTION AND CURIE TEMPERATURE

*First-principles* calculations of the thermodynamic properties of itinerant magnetic systems, via mapping[33,34] of the zero temperature band energy onto a classical Heisenberg model:

$$H_{\text{eff}} = -\sum_{i,j} J_{ij}\, \mathbf{e}_i \cdot \mathbf{e}_j \;, \tag{1}$$

has been discussed in detail in our previous publications.[35,36] Here $i,j$ are site indices, $\mathbf{e}_i$ is the unit vector pointing along the direction of the local magnetic moment at site $i$, and $J_{ij}$ is the exchange interaction between the moments at sites $i$ and $j$. The calculations are based on a mapping procedure due to Liechtenstein *et al.*[37–39] The method was later extended to random magnetic systems by Turek *et al.* , using CPA and the TB-LMTO method.[40] The exchange integral in Eq.(1) is given by

$$J_{ij} = \frac{1}{4\pi} \lim_{\epsilon \to 0^+} Im \int tr_L \left[ \Delta_i(z) g_{ij}^{\uparrow}(z) \Delta_j(z) g_{ji}^{\downarrow}(z) \right] dz \;, \tag{2}$$

where $z = E + i\epsilon$ represents the complex energy variable, $L = (l, m)$, and $\Delta_i(z) = P_i^\uparrow(z) - P_i^\downarrow(z)$, representing the difference in the potential functions for the up and down spin electrons at site '$i$'. $g_{ij}^\sigma(z)(\sigma = \uparrow, \downarrow)$ represents the matrix elements of the Green's function of the medium for the up and down spin electrons. For sublattices with disorder, this is a configurationally averaged Green's function, obtained via using the prescription of CPA. It should be noted that the spin magnetic moments are included in the above definition of $J_{ij}$. Positive and negative values of $J_{ij}$ imply FM and AFM couplings, respectively, between the atoms at sites $i$ and $j$.

Existence of the HM gap in spin polarized electronic densities of states does not guarantee that the substance is actually ferromagnetic (FM). The search for the ground magnetic state often needs to be guided by *ab initio* calculation of the exchange interactions between various atoms. In the above procedure outlined by Liechtenstein *et al.*,[37–39] exchange interactions are calculated by considering spin deviation from a reference state. Negative exchange interactions resulting from calculations based on a FM reference state would suggest instability of the assumed FM ground state. With this mind, we have computed the exchange interactions for the most interesting cases, i.e. those promising robust HM states. The results for the exchange interactions are shown in Figs.(3-5)

In Figs. 3 and 4 we show results for the cases with 75% doping with Cr and V for the RS and ZB structures, as this level of doping yields largest values of the minority spin and HM gaps. In Fig. 5 we consider the 25% Mn-doping case for the RS structure, the only Mn-doped case studied which shows the promise of half-metallicity. The solid lines (with circles) in these figures refer to the alloys with the equilibrium lattice parameters. In order to understand some trends, we have also considered lattice parameters above and/or below the equilibrium values. Ferromagnetic interactions are strongest in the Cr-doped ZB GeTe. The Cr-doping case is most promising, as in both RS and ZB structures FM interactions dominate, and these remain FM with changes in the lattice parameter. The next promising case is V-doping in the ZB structure, the RS counterpart showing strong antiferromagnetic (AFM) interactions, particularly at and around the equilibrium lattice parameter. These AFM interactions weaken on both sides of the equilibrium lattice parameter value and become FM only at much higher volume. Fig.5 shows that all interactions up to many neighbor shells are AFM, and then die off to zero. Hence the ground state cannot be FM. This conclusion needs to reinforced by examining the Lattice Fourier transformation of all the interactions. However, the preponderance of AFM interactions would dictate that the ground state is perhaps AFM or of complex magnetic structure. This issue is further explored in the next section. For the 25% Mn-doped solid the interactions are strongly AFM not only at the equilibrium lattice parameter, but also for a substantial range of the lattice parameter around equilibrium value. The interactions can become FM only
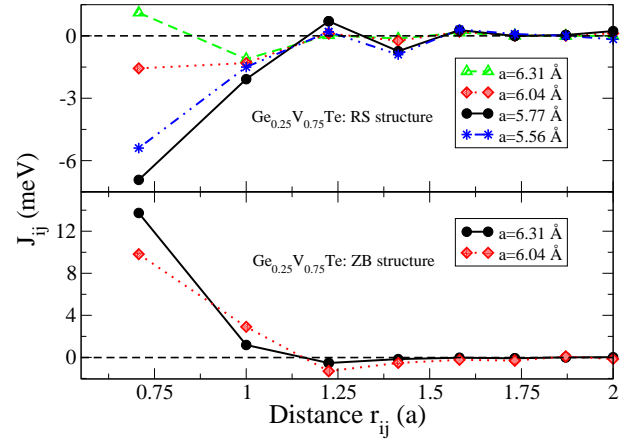


FIG. 3: (Color online) Exchange interaction between the V atoms in $Ge_{0.25}V_{0.75}Te$ as a function of interatomic distance expressed in units of lattice parameter $a$. Solid lines with solid circles show the



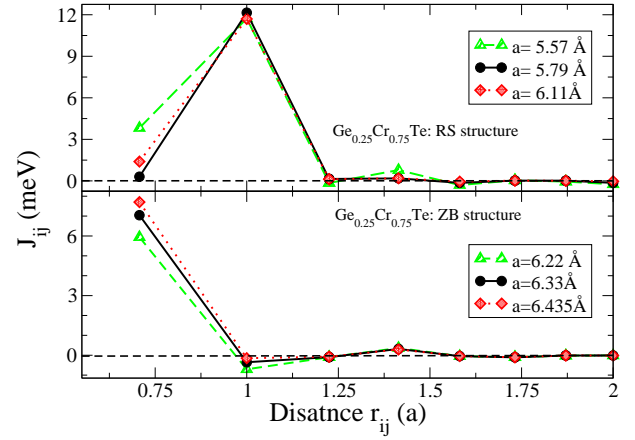FIG. 4: (Color online) Exchange interaction between the Cr atoms in $Ge_{0.25}Cr_{0.75}Te$ as a function of interatomic distance expressed in units of lattice parameter $a$. Solid lines with solid circles show the results for the equilibrium lattice parameters.

at unrealistically large lattice parameter, while compression would result in stronger AFM interactions. While our theoretical calculations suggest that 25% Mn-doping of the Ge-sublattice should lead to a ground state that is either AFM or of a more complex magnetic structure, some recent experimental results suggest ferromagnetism in these or similar Mn-doped compounds. Thus we will discuss the Mn-doping case separately in order to shed some light on the apparent discrepancy between theoretical results and the available experimental studies. In the following paragraphs we first present estimates of the Curie temperature for the Cr- and V-doped Ge-Te.

We have calculated the Curie temperature $T_c$ using both the mean-field approximation (MFA) and the more accurate random-phase approximation (RPA).[41] If the
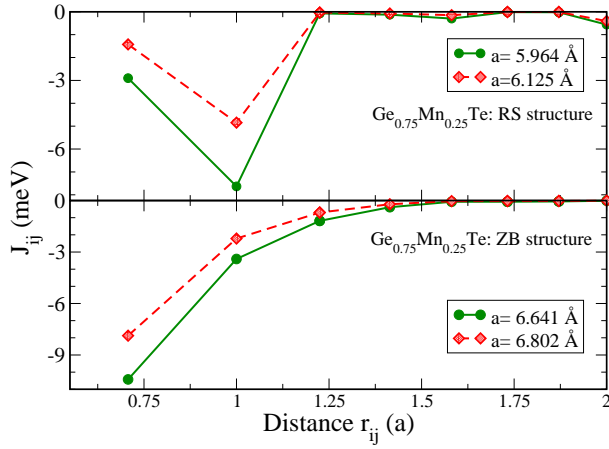
FIG. 5: (Color online) Exchange interaction between the Mn atoms in $Ge_{0.75}Mn_{0.25}Te$ as a function of interatomic distance expressed in units of lattice parameter $a$. Solid lines with solid circles show the results for the equilibrium lattice parameters.



FIG. 6: (Color online) $T_c$ (via RPA together with VCA) versus lattice parameter $a$ in $Ge_{1-x}X_xTe$ (X=V, Cr) alloys in ZB structure. The arrows indicate the values for the equilibrium lattice parameters for $x=0.75$

magnetic sublattice consists only of the magnetic atoms X, then in the MFA, the Curie temperature is given by

$$k_B T_c^{\mathrm{MFA}} = \frac{2}{3} \sum_{i \neq 0} J_{0i}^{\mathrm{X,X}}, \qquad (3)$$

where the sum extends over all the neighboring shells and involves the exchange interactions between the magnetic atoms $X$. MFA is known to grossly overestimate $T_c$. A much more improved description of finite-temperature magnetism is actually provided by the RPA. Again, if the magnetic sublattice consists only of the magnetic atoms X, then the RPA $T_c$ given by

$$(k_B T_c^{\mathrm{RPA}})^{-1} = \frac{3}{2} \frac{1}{N} \sum_{\mathbf{q}} [J^{\mathrm{X,X}}(\mathbf{0}) - J^{\mathrm{X,X}}(\mathbf{q})]^{-1}. \quad (4)$$

Here $N$ denotes the order of the translational group applied and $J^{\mathrm{X,X}}(\mathbf{q})$ is the lattice Fourier transform of the real-space exchange interactions $J_{ij}^{\mathrm{X,X}}$. In order to address the randomness in the Ge-TM sublattice, we have modified Eqs.(3) and (4) for our $Ge_{1-x}X_xTe$ alloys using virtual crystal approximation (VCA). This involves simply weighting the exchange integrals in Eq. (1) by $x^2$, where $x$ is the concentration of the X (TM) atoms. As a result, Tc's obtained from Eqs.(3) and (4) get multiplied by the same factor. In this way the problem is formally reduced to a nonrandom case. This approximation fails for low concentrations, below the percolation limit.[23] The error decreases monotonically for higher and higher concentrations. In general, the VCA results may somewhat overestimate the Curie temperature.

A problem arises in the computation of $T_c$ using either Eq.(3) or (4) when, in addition to the robust moments on the magnetic atoms, there are induced moments on
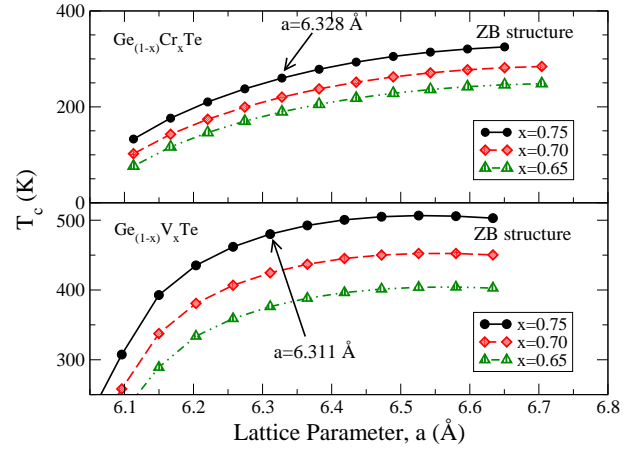
apparently non-magnetic atoms, interstitial spaces or, in case of the LMTO method, empty spheres. This problem has been discussed in detail in our previous publication[35] and references cited therein. As shown by Sandratskii *et al.*[33] the calculation of $T_c$ using RPA is considerably more involved even for the case where only one secondary induced interaction needs to be considered, in addition to the principal interaction between the strong moments. The complexity of the problem increases even for MFA, if more than one secondary interaction is to be considered. In our case, the induced moments are small and as such interactions involving non-magnetic atoms/spheres can be neglected in the first approximation. In addition, we are only interested in a rough estimation of $T_c$, the object being able to determine which doping would lead to a higher $T_c$ and hopefully be close to or above the room temperature. Our results, obtained by using the RPA and considering only the TM moments in Eq.(4), and further modified in the spirit of VCA, are summarized Figs. 6 and 7. We show $T_c$ as a function of the lattice parameter for various relevant levels of doping. The equilibrium lattice parameter values are indicated with arrows. Doping with Cr or V in the ZB structure for doping levels around 75% is promising, with V-doping showing higher $T_c$ values than Cr-doping. V-doping in RS structure is not recommended, while Cr-doping in RS structure leads to reasonably high values of $T_c$ for all levels of doping higher than 50%. In a previous publication[36] we have already presented a comparison of pure CrTe in ZB and RS structures, pointing out various advantages of considering RS CrTe over ZB CrTe from the viewpoint of spintronics applications.
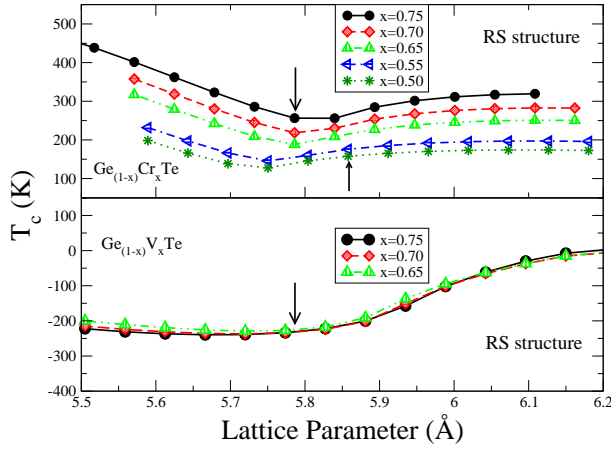
FIG. 7: (Color online) $T_c$ (via RPA together with VCA) versus lattice parameter $a$ in $Ge_{1-x}X_xTe$ (X=V, Cr) alloys in RS structure. The arrows indicate the values for the equilibrium lattice parameters for $x=0.75$, and 0.50 for $Ge_{1-x}Cr_xTe$ and $x=0.75$ for $Ge_{1-x}V_xTe$.

TABLE V: Energy differences between ferromagnetic (FM) and various antiferromagnetic (AFM) configurations of RS and ZB $Ge_3Mn_1Te_4$. The energies of the AFM unit cells are compared with 2 FM unit cells. MO stands for magnetic order. The energy difference $\Delta E$ of the AFM configurations with respect to the FM, in the last column, are given per formula unit.

| MO | Energy (eV) | $\Delta E$ (meV) |
|---|---|---|
| RS structure: | | |
| FM | -942305.912 | 0 |
| AFM001 | -1884611.922 | -49 |
| AFM110 | -1884611.981 | -79 |
| AFM111 | -1884612.033 | -105 |
| ZB Structure: | | |
| FM | -942304.475 | 0 |
| AFM001 | -1884608.979 | -14 |
| AFM110 | -1884609.006 | -28 |
| AFM111 | -1884609.018 | -33 |

## V. THE CASE OF Ge-Mn-Te

Our results for the alloys $Ge_3Mn_1Te_4$ and $Ge_{0.75}Mn_{0.25}Te$ need to be examined carefully in the context of the existing experimental studies, many of which claim evidence of ferromagnetism over a wide range of Mn concentration with $T_c$'s up to 100-200 K. Our LMTO-ASA-based exchange interactions indicate that the ground state should not be FM, at least for the 25% Mn concentration case studied by us. These results are based on LDA. So first we have checked that the use of GGA and more accurate full-potential results are not drastically different. In Table V we show the results for the FP-LAPW (Wien2k) results obtained with GGA for the ordered $Ge_3Mn_1Te_4$ alloy. These results show that for both RS and ZB structures the AFM state energies are lower than the FM state energies, with the AFM [111] configuration having the lowest energy among the three AFM configurations considered. The AFM [111] unit cells of $Ge_3Mn_1Te_4$, doubled with respect to the conventional FM unit cells, are shown in Fig. 8.

In the RS structure the energy difference of the AFM configurations, in particular the [111] case, is larger than for the ZB case. To examine the magnetic structure of the ground state we also consider the lattice Fourier transform of the exchange interaction between the Mn atoms:

$$J(\mathbf{q}) = \sum_{\mathbf{R}} J_{0\mathbf{R}}^{Mn,Mn} \exp(i\mathbf{q} \cdot \mathbf{R});  \quad (5)$$

where $\mathbf{q}$ is a wave vector in the BZ of the fcc lattice. A maximum at the L point would point to the ground state being AFM [111], while that at the $\Gamma$ point would indicate the ground state being FM. We have examined the ground state magnetic structure via $J(\mathbf{q})$ using both FM and the disordered local moment (DLM)[42,43] reference

states. Within the Stoner model, a nonmagnetic state above the Curie temperature $T_c$ is characterized by the vanishing of the local moments in magnitude. This obviously flawed description of the nonmagnetic state can be improved by using the DLM model, where the local moments remain nonzero in magnitude above $T_c$, but disorder in their direction above $T_c$ causes global magnetic moment to vanish. For Mn this is known to be a good approximation. Within the collinear magnetic model, where all local axes of spin-quantization point in the same direction, DLM can be treated as a binary alloy problem.[35] The results for the RS structure, obtained by using the FM and DLM reference states are shown in sections (a) and (b) of Fig. 9, respectively. Exchange interactions based on both FM and DLM reference states indicate that the ground state magnetic structure of RS $Ge_{0.75}Mn_{0.25}Te$ is AFM [111].

However, the situation for ZB $Ge_{0.75}Mn_{0.25}Te$ is not so clear. Both DLM and FM reference states yield $J(\mathbf{q})$ curves with a broad maximum enclosing the symmetry points X, W, and K. In addition, the values of $J(\mathbf{q})$ at these points is marginally higher than that at the L point (sections (a) and (b) of Fig. 10). What is certain is that the ground state is not FM, with $J(\mathbf{q})$ being a minimum at the $\Gamma$-point. Thus the ground state for ZB $Ge_{0.75}Mn_{0.25}Te$ may involve a complex magnetic structure or the substance may enter a spin-glass state at low temperatures. In order to ensure that our results do not suffer from a convergence problem, we have looked at the $J(\mathbf{q})$ values as a function of increasing shells of neighbors. The results for ZB $Ge_{0.75}Mn_{0.25}Te$ with FM reference state are shown in section (c) of Fig.10. Results for 10 shells of neighbor are indistinguishable from those for 63 shells considered in all our calculations, indicating that our results are well-converged.
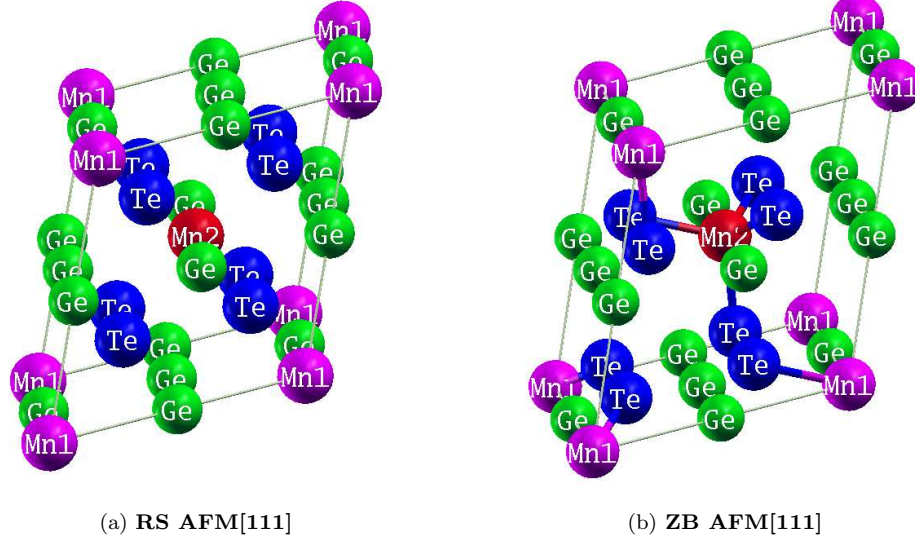
(a) **RS AFM[111]**  (b) **ZB AFM[111]**

FIG. 8: (Color online) Unit cells of $Ge_3Mn_1Te_4$ in AFM [111] configuration.
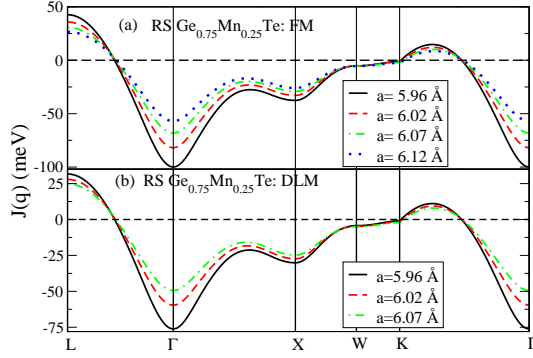


FIG. 9: (Color online) Lattice Fourier transform of Mn-Mn interactions for various lattice parameters in RS $Ge_{0.75}Mn_{0.25}Te$ for (a) FM and (b) DLM reference states. Solid lines represent the results for the equilibrium lattice parameter.

FIG. 10: (Color online) Lattice Fourier transform of Mn-Mn interactions in ZB $Ge_{0.75}Mn_{0.25}Te$ for (a) FM and (b) DLM reference states and for various lattice parameters. Section (c) shows variation with respect to the number of neighbor shells. Results for 10 shells of neighbors are indistinguishable from those of 63 shells used in all our calculations. Solid lines in (a) and (c) represent the results for the equilibrium lattice parameter.

Experimentally, $Ge_{1-x}Mn_xTe$ alloys, with X=Cr, Mn, Fe have been reported to exhibit ferromagnetic behavior[11–21] over wide range of the concentration $x$. The structure of these compounds, grown as thin films, is usually found to be RS or small deviations from this. For $Ge_{1-x}Mn_xTe$ the structure is found to be rhombohedrally distorted NaCl for small Mn concentrations, with the distortion vanishing for $x > 0.18$.[1] These studies also report presence of carriers in the samples, with transport measurements most often indicating p-type carriers,[1,2,7,15] independent of temperature. Fukuma and co-workers identify the carriers as holes.[1,7,15] Depending on carrier concentration, brought about by varying Mn concentration or hydrostatic pressure, $T_c$ may vary non-monotonically.[1,18] Highest reported $T_c$ is around 130-140 K for Mn concentration $x$ slightly over 50% in the Ge-
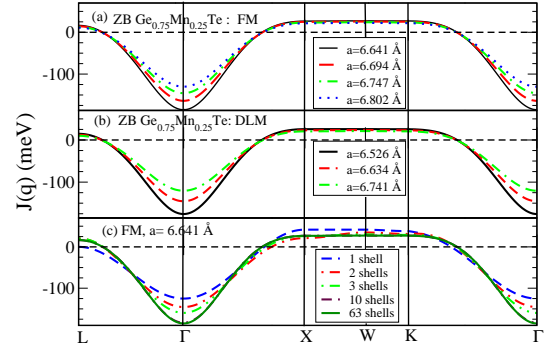
Mn sublattice, and for $x = 0.25$ $T_c$ is $\sim 70$ K.[1] Other authors report $T_c$ values more or less in the same range depending on Mn concentration.[2,7,16] $T_c$ values reported for RS or nearly RS $Ge_{1-x}Cr_xTe$ films are higher.[5] Note that the lattice parameters reported for $x = 0.24$ and 0.55 in $Ge_{1-x}Mn_xTe$ are 5.939 and 5.895 Å, respectively, which compare well with our calculated values 5.964 and 5.914 Å, for $x = 0.25$ and 0.50, respectively (Table I).

Our zero temperature results indicate that exactly at the concentration $x=0.25$, $Ge_{1-x}Mn_xTe$ should be either a semiconductor with small gap or at best a zero gap semiconductor, in both RS and ZB structures. The mag-

netic structure of the ground state in this case is not FM, it is either AFM or more complex. At finite temperatures, free carriers in the conduction band and holes in the valence band are expected and the number of such carriers may be significant in view of the fact that the gap is close to zero. However, it is believed that there are also a large number of carriers, mainly holes, with temperature-independent concentration.[2] RS GeTe is reported to be a narrow gap semiconductor with a band gap of about 0.2 eV.[44] Its very high $p$-type conduction is ascribed to large cation (Ge) vacancies,[15,44–46] which seem to dominate over transport due to thermally excited carriers. We have thus decided to explore this issue, in the framework of our zero temperature formalism, in several ways. Guided by the fact that experiments indicate presence of uncompensated carriers, with temperature-independent concentrations, we first explore the effects of such carriers using the simplest possible approach. The easiest thing for us is to find the change in Mn-Mn exchange interaction by moving the Fermi energy up (simulating holes) or down (simulating electrons). This is a one step non-self-consistent (frozen potential) calculation, in the spirit of the rigid band model. After self-consistency has been achieved for the equilibrium lattice parameter, exchange interactions are calculated for the self-consistent potential and the correct Fermi energy, and then also for the same potential but assuming the Fermi energy to be slightly higher/lower to simulate holes/electrons. The Fermi energy coming out from the self-consistent calculation for the equilibrium lattice parameter is simply moved up or down by 0.136/0.68 eV (0.01/0.05 Ry). In Fig.11 we show this change for both ZB and RS structure $Ge_{0.75}Mn_{0.25}Te$ and $\Delta(E_F) = \pm 0.68$ eV (0.05 Ry). In both cases, i.e. Fermi energy changed by $\pm 0.68$ eV, there is an increase in the Mn-Mn interaction. In Fig.12 we compare the results of changing he Fermi energy by 0.136 eV and 0.68 eV in RS $Ge_{0.75}Mn_{0.25}Te$ for two different lattice parameters. This indicates that both electron- and hole-doping of the system would be an efficient way to drive it toward ferromagnetism. Of course, hole- and electron-doping can be simulated in other ways as well, for example, by changing the effective valence of the atoms. This can be done by changing the valence of the magnetic or the nonmagnetic atoms. In Fig.13 we show the effect of altering the valence of Mn atoms from 7 to 6.8, 6.9 and 7.1 for different lattice parameters. This is equivalent to studying the effect of alloying of Mn with other elements to the left or right in the same row of the periodic table using virtual crystal approximation (VCA). These calculations are self-consistent, as opposed to the above results with rigidly shifted Fermi levels, but may suffer from the weaknesses of VCA. We have also included the case where Mn concentration in the Ge-sublattice is reduced from 25% to 22% and the remaining 3% of the sites on this sublattice are left vacant. In all these calculations it is the magnetic atom Mn, whose concentration is effectively altered to create the electrons or holes. Next, we explore
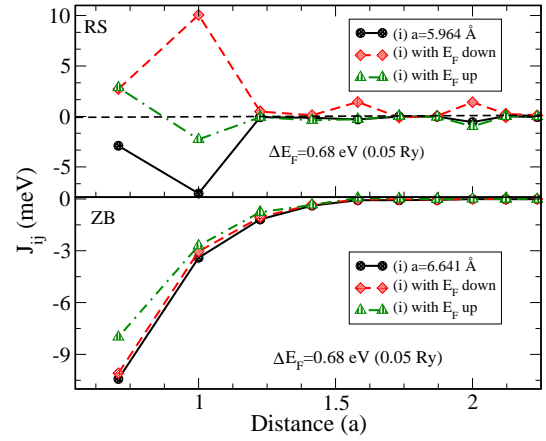


FIG. 11: (Color online) Change (non self-consistent result) in Mn-Mn exchange interactions in RS and ZB $Ge_{0.75}Mn_{0.25}Te$ computed by moving the Fermi energy (rigid shift) by 0.68 eV (0.05 Ry) up or down with respect to the result of the self-consistent calculation for the alloy. Solid lines with solid circles are the results of self-consistent calculations for the equilibrium lattice
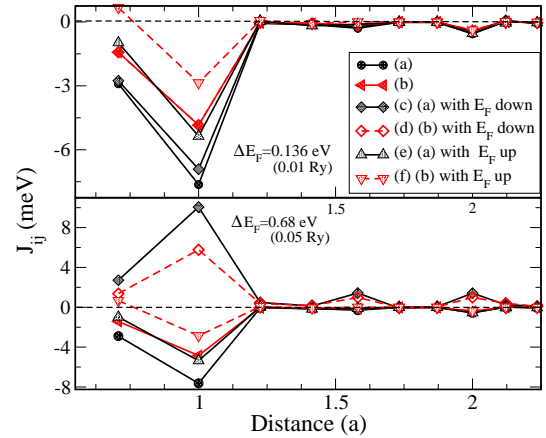


FIG. 12: (Color online) Change (non self-consistent result) in Mn-Mn exchange interactions in RS $Ge_{0.75}Mn_{0.25}Te$ computed by moving the Fermi energy (rigid shift) by 0.136 eV (0.01 Ry) and 0.68 eV (0.05 Ry) up or down with respect to the result of the self-consistent calculation for the alloy. Results are shown for two different lattice parameters: (a) equilibrium lattice parameter 5.964 Å, (b) expanded lattice parameter 6.125 Å.

the effect of creating holes or electrons by keeping the concentration of Mn atoms fixed at 25%.

We study separately the effect of introducing holes by doping the Ge-sublattice and the Te-sublattice. To create holes in the Ge-sublattice, we replace some of the Ge-atoms with Cu, and to create holes in the Te-sublattice we replace some Te-atoms with Sn or simply vacancies. Results are shown in Figs. 14 and 15. Fig. 14 shows
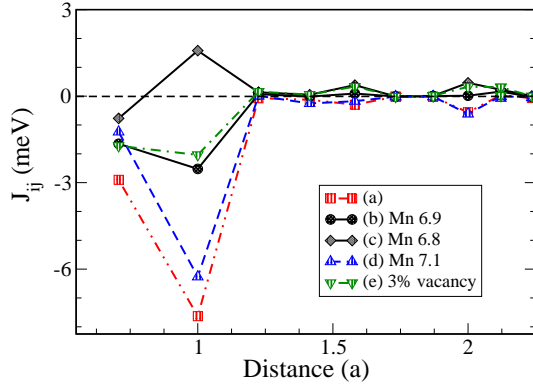
FIG. 13: (Color online) Change in Mn-Mn exchange interactions brought about by change in carrier concentration in various different ways in RS $Ge_{0.75}Mn_{0.25}Te$. (a) Self-consistent result for equilibrium lattice parameter 5.964Å, (b) same as (a), but by assigning 6.9 electrons to Mn atoms, thus simulating hole-doping, (c) same as (b), but by assigning 6.8 electrons to Mn atoms, thus simulating larger hole concentration, (d) same as (b) or (c), except that Mn valence has been moved to 7.1, simulating electron-doping, (e) self-consistent result for equilibrium lattice parameter, but by replacing 3% of the atoms in the Ge-Mn sublattice by empty spheres (vacancies).
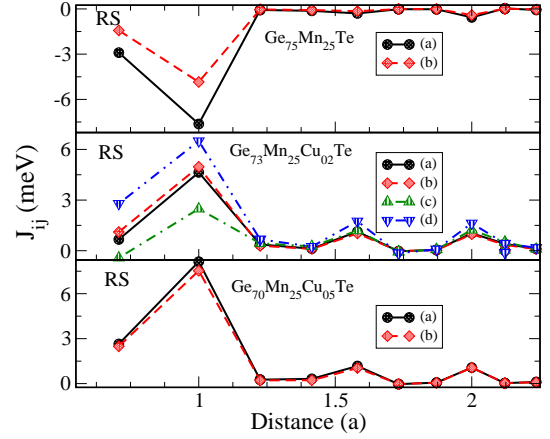


FIG. 14: (Color online) Mn-Mn exchange interactions in RS Ge-Mn-Te, obtained by putting 2% and 5% Cu in the Ge-Mn sublattice. Cu-atoms randomly replace the Ge-atoms, thus keeping the Mn concentration fixed at 25%. The legends (a)-(d) refer to different lattice parameters: (a) equilibrium $Ge_{0.75}Mn_{0.25}Te$ lattice parameter 5.964 Å, (b) expanded lattice parameter 6.125 Å, (c) and (d) contracted lattice parameters 5.750 Å and 5.534 Å, respectively.

the effect of replacing some of the Ge atoms with Cu, thus creating holes. Results show the effect of increasing hole-concentration as well as the effect of changing the lattice parameter or the volume per atom. We have considered only the RS case, as all the available experimental results are for this structure. It is clear that even a reasonably low level of Cu-doping of the Ge-sublattice can substantially increase the Mn-Mn exchange interaction, changing it from negative to positive and explaining the observed ferromagnetism of $Ge_{1-x}Mn_xTe$ thin films. Fig. 15 shows the effect of creating holes via doping the Te-sublattice with Sn or creating vacancies in this sublattice. Again, there is a change in the Mn-Mn interaction in the direction of ferromagnetism (decreasing antiferromagnetic interactions).

## VI.  SUMMARY OF RESULTS AND CONCLUSIONS

We have examined theoretically the possibility of half-metallic ferromagnetism in bulk $Ge_{1-x}TM_xTe$ alloys, with TM being the transition metals V, Cr and Mn. FP-LAPW calculations reveal the possibility of half-metallicity for some of the ordered alloys. For these cases we have calculated the exchange interactions and the Curie temperatures. The later calculations apply to cases where the Ge and the TM atoms occupy randomly the Ge-sublattice. The effect of this disorder is taken into account using the CPA. Ferromagnetic interactions

are strongest in the Cr-doped ZB GeTe. The Cr-doping case is most promising, as in both RS and ZB structures FM interactions dominate, and these remain FM with changes in the lattice parameter. The next promising case is V-doping in the ZB structure, the RS counterpart showing strong antiferromagnetic (AFM) interactions, particularly at and around the equilibrium lattice parameter. These AFM interactions weaken on both sides of the equilibrium lattice parameter value and become FM only at much higher volume. Our calculations for TM=Mn and $x=0.25$ shows the substance to be AFM (for the ordered as well as disordered compounds, with the gap being narrower in the disordered case). We show that this AFM behavior is linked to the substance being a narrow/zero gap semiconductor/semimetal at this Mn concentration. We further establish that the presence of uncompensated carriers should drive the material toward ferromagnetism. The origin of these carriers could be vacancies, impurity atoms, and/or structural imperfections. In fact both Ge-Te and $Ge_{1-x}TM_xTe$ samples are known to have large number of holes ($p$-type carriers) due to cation(Ge) vacancies.[15,44–46] A comparison of the results in Figs. 14 and 15 clearly shows that holes in the Ge-Mn sublattice is much more effective in driving the system to ferromagnetism than the holes in Te-sublattice. This seems to be consistent with the experimental observation that all ferromagnetic films of $Ge_{1-x}TM_xTe$ have a large number of temperature-independent p-type carriers, associated with vacancies in the Ge sublattice. The calculated exchange interactions due to carriers originating from these causes are sufficient to account for the observed ferromagnetism in thin films of $Ge_{1-x}Mn_xTe$.
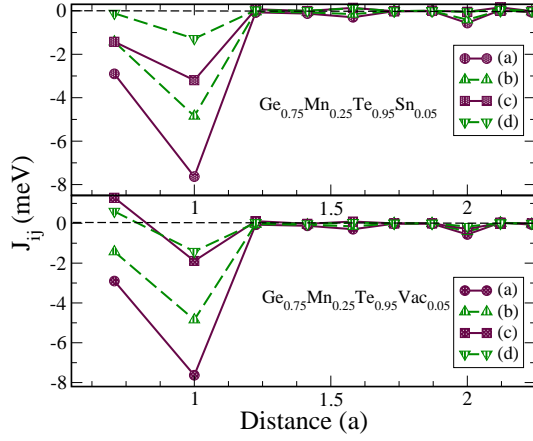
FIG. 15: (Color online) Mn-Mn exchange interactions in RS $Ge_{0.75}Mn_{0.25}Te_xZ_{1-x}$, where Z stands for Sn-atoms or vacancies. Sn-atoms or vacancies occupy random positions solely in the Te-sublattice. Legends: (a) $x$=1.0, a= 5.964 Å, (b) $x$=1.0, a=6.286 Å, (c) $x$=0.95, a= 5.964 Å, (d) $x$=0.95, a=6.286 Å.

Our results for the exchange interactions are consistent with experiments in that the highest $T_c$ reported so far seem to be for thin films of $Ge_{1-x}Cr_xTe$. Some differences between our calculated results and the experiments could be ascribed to the fact that our calculations are for bulk alloys, while experimental results are mostly for thin films. For example, distortions with respect to the bulk structures may be present in thin films, in addition to the fact that the lattice parameters of the thin films are usually larger than their bulk counterparts.[7]

* author to whom correspondence should be sent:sbose@brocku.ca

[1] Y. Fukuma, T. Murakami, H. Asada, and T. Koyanagi, Physica E **10**, 273 (2001).
[2] Y. Fukuma, H. Asada,, J. Miyashita, N. Nishimura, and T. Koyanagi, J. Appl. Phys. **93**, 7667 (2003).
[3] Y. Fukuma, N. Nishimura, F. Odawara, H. Asada, and T. Koyanagi, J. Supercond: Incorp. Nov. Magn., **16**, 71 (2003).
[4] Y. Fukuma, T. Taya, S. Miyawaki, T. Irisa, H. Asada, and T. Koyanagi, J. Appl. Phys. **99**, 08D508 (2006).
[5] Y. Fukuma, H. Asada, T. Taya, T. Irisa, and T. Koyanagi, Appl. Phys. Lett. **89**, 152506 (2006).
[6] Y. Fukuma, H. Asada, and T. Koyanagi, Appl. Phys. Lett. **88**, 032507 (2006).
[7] Y. Fukuma, H. Asada, S. Miyawaki, T. Koyanagi, S. Senba, K. Goto, and H. Sato, Appl. Phys. Lett.**93**, 252502 (2008).
[8] W.Q. Chen, S.T. Lim, C.H. Sim, J.F. Bi, K.L. Teo, T. Liew, and T.C. Chong, J. Appl. Phys. **104**, 063912 (2008).
[9] Y-H Zhao, W-H Xie, L-F Zhu, and B-G Liu, J. Phys.: Condens. Matter **18**, 10259 (2006).
[10] A. Ciucivara, B.R. Sahu, and L. Kleinman, Phys. Rev. B **75**, 241201(R) (2007).
[11] Y. Fukuma, H. Asada, N. Moritake, T. Irisa, and T. Koyanagi, Appl. Phys. Lett. **91**, 092501 (2007).
[12] S. T. Lim, J. F. Bi, K. L. Teo, Feng Y. P, T. Liew,and T. C. Chong, Appl. Phys. Lett. **95**, 072510 (2009).
[13] R. T. Lechner *et al.* , Appl. Phys. Lett. **97**, 023101 (2010).
[14] F. Tong, J. H. Hao, Z. P. Chen, G. Y. Gao, and X. S. Miao, Appl. Phys. Lett. **99**, 081908 (2011).
[15] Y. Fukuma *et al.* , J. Appl. Phys. **103**, 053904 (2008).
[16] E. A. Zvereva *et al.* , J. Appl. Phys. **108**, 093923 (2010).
[17] S. T. Lim, J. F. Bi, K. L. Teo, and T. Liew, J. Appl. Phys. **109**, 07C314 (2011).
[18] S. T. Lim, J. F. Bi, Lu Hui, and K. L. Teo, J. Appl. Phys. **110**, 023905 (2011).

[19] S. T. Lim, L. Hui, J. F. Bi, and K. L. Teo, J. Appl. Phys. **110**, 113916 (2011).
[20] M. Hassan *et al.* , J. Cryst. Growth. **323**, 363 (2011).
[21] L. Kilanski *et al.* , Phys. Rev. B **82**,094427(2010).
[22] K. Sato *et al.* , Rev. Mod. Phys. **82**, 1633 (2010).
[23] L. Bergqvist, O. Eriksson, J. Kudrnovský, V. Drchal, P. Korzhavyi, and I. Turek, Phys. Rev. Lett. **93**, 137202 (2004).
[24] P. Blaha, K. Schwarz, G. Madsen, D. Kvasnicka, J. Luitz, WIEN2k, An Augmented Plane Wave Plus Local Orbitals Program for Calculating Crystal Properties, Vienna University of Technology Inst. of Physical and Theoretical, Vienna, Austria, 2008; P. Blaha, K. Schwarz, P. Sorantin, Comput. Phys.Commun. **59**, 399 (1990).
[25] J. Kudrnovský and V. Drchal, Phys. Rev. B **41**, 7515 (1990).
[26] I. Turek, V. Drchal, J. Kudrnovský, M. Šob, and P. Weinberger, *Electronic Structure of Disordered Alloys, Surfaces and Interfaces* (Kluwer, Boston-London-Dordrecht, 1997).
[27] P. Hohenberg and W. Kohn, Phys. Rev. **136**, B864 (1964); W. Kohn and L.J. Sham, Phys. Rev. **140**, A1133 (1965).
[28] J.P. Perdew, Y. Wang, Phys. Rev. B **45**, 13244 (1992).
[29] J.P. Perdew, K. Burke and M. Ernzerhof, Phys. Rev. Lett. **77**, 3865 (1996).
[30] H.J. Monkhorst, J.D. Park, Phys. Rev. B **13**, 5188 (1976).
[31] F.D. Murnaghan, Proc. Natl. Acad. Sci. USA **30**, 5390 (1944).
[32] S.H.Vosko, L. Wilk, and M. Nusair, Can. J. Phys. **58**, 1200 (1980).
[33] L.M. Sandratskii, R. Singer, and E. Sasioğlu, Phys. Rev. B **76**, 184406 (2007).
[34] M. Pajda, J. Kudrnovský, I. Turek, V. Drchal, and P. Bruno, Phys. Rev. B **64**, 174402 (2001).
[35] S.K. Bose and J. Kudrnovský, Phys. Rev. B **81**, 054446 (2010).
[36] Y. Liu, S.K. Bose, J. Kudrnovský, Phys. Rev. B **82**, 094435

(2010).

[37] A.I. Liechtenstein, M.I. Katsnelson and V.A. Gubanov, J. Phys.F: Met.Phys. **14**, L125 (1984).

[38] A.I. Liechtenstein, M.I. Katsnelson and V.A. Gubanov, Solid. State. Commun. **54**, 327 (1985).

[39] V.A. Gubanov, A.I. Liechtenstein, A.V. Postnikov *Magnetism and the electronic structure of crystals*, edited by M. Cardona, P. Fulde, K. von Klitzing, H.-J. Queisser (Springer, Berlin, 1992).

[40] I. Turek, J. Kudrnovský, V. Drchal, and P. Bruno, Philos. Mag. **86**, 1713 (2006).

[41] C.S. Wang, R.E. Prange, and V. Korenman, Phys. Rev. B **25**, 5766 (1982).

[42] V. Heine, J.H. Samson, and C.M.M. Nex, J. Phys. F: Met. Phys. **11**, 2645 (1981).

[43] V. Heine and J.H. Samson, J. Phys. F: Met. Phys. **13**, 2155 (1983).

[44] R. Tsu, W.E. Howard, and L. Esaki, Phys. Rev. **172**, 779 (1968).

[45] J.E. Lewis, Phys. Status Solidi B **59**, 367 (1973).

[46] D.H. Damon, M.S. Lubell, and R. Mazelsky, J. Phys. Chem. Solids **28**, 520 (1967).